ELSEVIER

www.elsevier.nl/locate/ica

Volume 297, Numbers 1–2, January 2000

Inorganica Chimica Acta

Contents

Preface xvii

Articles

Raquel L. Lieberman, Avi Bino, Nitza Mirsky, David A. Summers, Robert C. Thompson

Inorg. Chim. Acta 297 (2000) 1

Synthesis, structure and magnetic properties of a chromium(III)–nicotinamide complex $[Cr_3O(O_2CCH_3)_6(na)_3]^+$ (na = nicotinamide)

The compound $[Cr_3O(O_2CCH_3)_6(na)_3]\cdot PF_6\cdot 3CH_3CN$ (na = nicotinamide) has been prepared and structurally characterized. The three N-bonded na ligands occupy axial positions at the corners of the triangular basic chromium acetate with Cr–N(na) bond distances ranging from 2.121(8) to 2.128(8) Å. Each two Cr_3 units in the cell are hydrogen-bonded through two na ligands. The three Cr(III) ions are antiferromagnetically coupled with $J = -10.4\ cm^{-1}$ and there was no evidence for intermolecular magnetic exchange between the two Cr_3O centers.

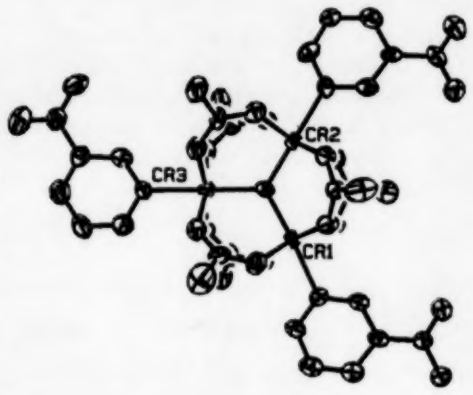

F. Albert Cotton, Lee M. Daniels, Glenn T. Jordan IV, Carlos A. Murillo, Isabel Pascual

Inorg. Chim. Acta 297 (2000) 6

Structural variations in the ligands around a simple oxo-centered building block, the tetrahedral $[M_4O]^{6+}$ unit, M = Mn and Fe

Hydrolysis of divalent *N′,N′*-dipyridyl complexes of Fe and Mn produce compounds with an $[M_4(\mu_4\text{-}O)]^{6+}$ core. The potentially tridentate ligand gives rise to an interesting form of isomerism.

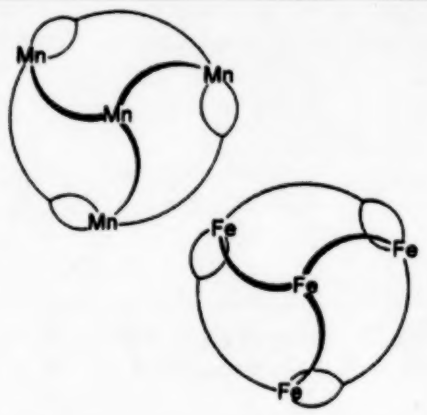

Kathleen M. Vogel, Pawel M. Kozlowski, Marek Z. Zgierski, Thomas G. Spiro

Inorg. Chim. Acta 279 (2000) 11

Role of the axial ligand in heme–CO backbonding; DFT analysis of vibrational data

The Fe–CO and C–O stretching frequencies are negatively correlated for a series of five-coordinate CO adducts Fe^{II} porphyrins, due to backbonding, but the slope is half that of six-coordinate adducts. The effect is reproduced by DFT calculations which show that the Fe–CO bond is lengthened by axial donoor ligands, thereby increasing the Fe–CO sensitivity to backbonding changes.

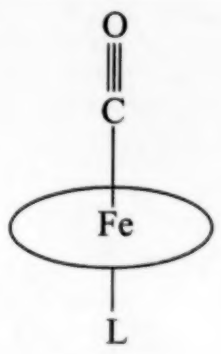

Tomoaki Tanase, Chiharu Inoue, Emi Ota, Shigenobu Yano, Masashi Takahashi, Masuo Takeda

Inorg. Chim. Acta 297 (2000) 18

Tetranuclear iron(III) complexes with a planar (μ-oxo)(μ-hydroxo)bis(μ-alkoxo)bis(μ-carboxylato)-tetrairon core derived from hydrolysis of carboxylic acid amides by diiron(III) center

Reactions of $Fe(NO_3)_3\cdot 9H_2O$ with 0.5 equiv. of 2-hydroxy-1,3-diaminopropane *N,N,N′,N′*-tetraacetic acid (H_5dhpta) in a mixed solvent of water and *N,N*-dimethyl carboxylic acid amide (*N,N*-Me_2NCOR) gave the tetrairon(II) complexes $(Me_2NH_2)_4[Fe_4(dhpta)_2(\mu\text{-}O)(\mu\text{-}OH)(O_2CR)_2](NO_3)$ (R = H (**1a**), CH_3 (**1b**), CH_2CH_3 (**1c**)), through amide hydrolysis on diiron(III) center.

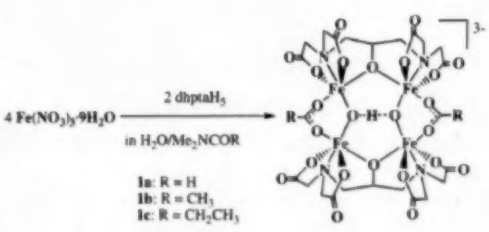

Elsevier Science S.A.

Andreja Bakac, Wei-Dong Wang

Inorg. Chim. Acta 297 (2000) 27

Generation of a macrocyclic Cr(V) complex and its reactivity toward organic and inorganic reductants and DNA

One-electron reduction of L^1CrOO^{2+} (L^1 = cyclam) yields the hydroperoxo complex, L^1CrOOH^{2+}. In a first-order follow-up process, $k = 0.19\ s^{-1}$, the hydroperoxide is converted to an oxochromium(V) complex, L^1CrO^{3+}, which is a potent oxidant and reacts rapidly with a number of inorganic and organic reductants and with DNA.

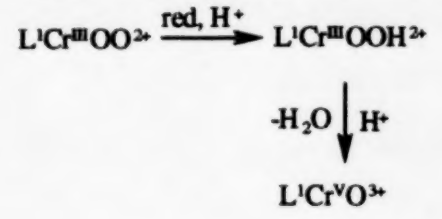

Hing C. Wong, Kazuo Shinozuka, Giovanni Natile, Luigi G. Marzilli

Inorg. Chim. Acta 297 (2000) 36

Second-sphere 'communication' between two *cis*-bound guanine nucleotides. Factors influencing conformations of dynamic adducts of *cis*-type platinum anticancer drugs with guanine nucleotides as deduced by circular dichroism spectroscopy

Intramolecular phosphate–N1H hydrogen bonds formed between two *cis* **G** nucleotides favor the ΔHT and ΛHT conformers for the 3′-GMP and 5′-GMP adducts, respectively. The dominance of one chiral form accounts for the characteristic enhanced CD signal long known for GMP adducts of cisplatin.

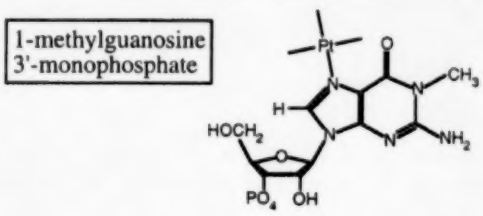

David A. Williamson, Bruce E. Bowler

Inorg. Chim. Acta 297 (2000) 47

Porphyrin to quinone electron transfer across a depsipeptide which forms an α-helical turn

A porphyrin linked to a quinone via a three residue depsipeptide, L-prolone-L-lactate-L-lactate has been used to investigate the effect of a protein folding interaction on electron transfer rates through a protein medium. Infrared and NMR methods demonstrate the presence of an α-helical turn. Porphyrin to quinone electron transfer ($k_{et} = 5.6 \pm 0.3 \times 10^8\ s^{-1}$) is very efficient in this compound.

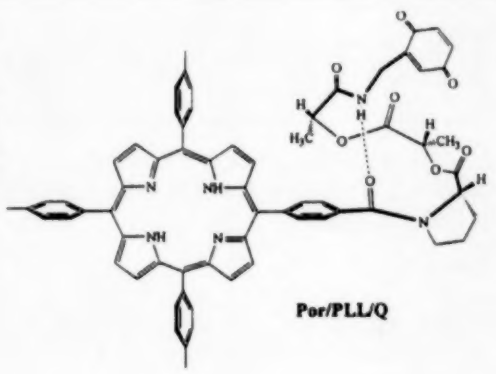

Anna Ericson, Yelena Iljina, Jason L. McCary, Robert S. Coleman, Sofi K.C. Elmroth

Inorg. Chim. Acta 297 (2000) 56

Reactions of $Pd(dien)Cl^+$ with thione-containing nucleosides, nucleotides and oligonucleotides: increase of both enthalpy and entropy of activation in the DNA-environment

Reactions of the labile complex $Pd(dien)Cl^+$ with the non-charged bases ^{s4}U and ^{s6}I are accelerated by a factor of 2–4 after incorporation into the middle of a 17-*mer* single-stranded DNA oligomer.

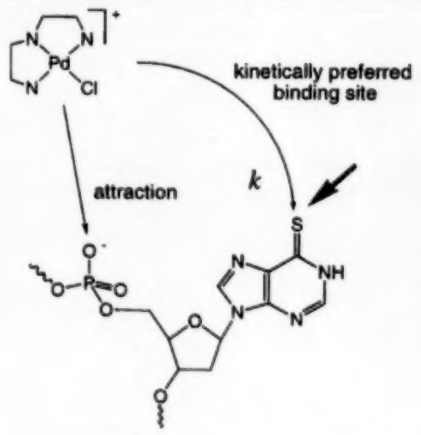

Ken Sakai, Yasushi Tomita, Takuma Ue, Koji Goshima, Masakatsu Ohminato, Taro Tsubomura, Kazuko Matsumoto, Kenji Ohmura, Kazuyuki Kawakami

Inorg. Chim. Acta 297 (2000) 64

Syntheses, antitumor activity, and molecular mechanics studies of *cis*-$PtCl_2(pzH)_2$ (pzH = pyrazole) and related complexes. Crystal structure of a novel Magnus-type double-salt $[Pt(pzH)_4][PtCl_4]$-[*cis*$PtCl_2(pzH)_2]_2$ involving two perpendicularly aligned 1D chains

A novel 1D compound $[Pt(pzH)_4]$-$[PtCl_4][cis\text{-}PtCl_2(pzH)_2]_2$ (**1**) has been prepared as a side product of *cis*-$PtCl_2(pzH)_2$ (**2**), and structurally characterized. Compound **1** possesses an intriguing intersecting framework. The in vitro antitumor activity of **2** toward some human cancer lines is found to be comparable to that of *cis*-$PtCl_2(NH_3)_2$. AMBER-based molecular mechanics calculations suggest the importance of hydrogen-bond formation between the NH(pzH) units and DNA.

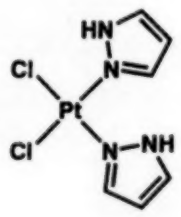

Stephen U. Dunham, Edwin H. Abbott

Inorg. Chim. Acta 297 (2000) 72

A nuclear magnetic resonance investigation of water exchange reactions and *trans* to *cis* isomerization for diaqua and dihydroxobis-(oxalato) and bis(malonato)platinum(IV) complexes

Isotopic shifts in ^{195}Pt NMR spectra have been used to study water exchange kinetics for the Pt(IV) oxalato complex, $[Pt(H_2O)_2(Ox)_2]$. Water exchange rates indicate that the direct substitution of a coordinated water with a Pt(II) oxalato complex, $[Pt(Ox)_2]^{2-}$, is too slow to account for the formation of one-dimensional metal–metal bonded Pt–oxalate polymers.

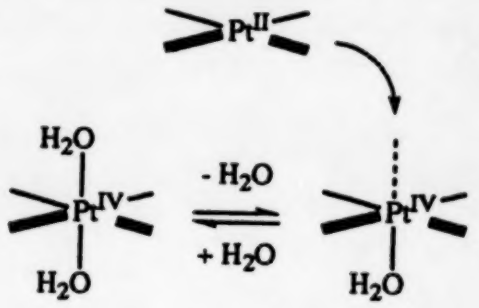

JudithAnn R. Hartman, Richard W. Vachet, John H. Callahan

Inorg. Chim. Acta 297 (2000) 79

Gas, solution, and solid state coordination environments for the nickel(II) complexes of a series of aminopyridine ligands of varying coordination number

The binding geometries in the solid, solution, and gas phases for nickel(II) complexes with a series of aminopyridine ligands were determined using magnetic susceptibility, spectroscopy, electrochemistry, and analyses of gas phase ion–molecule reactions in a mass spectrometer. Comparison of gas phase structures to condensed phase structures gives insight about the inherent fit between each ligand and the nickel(II) ion.

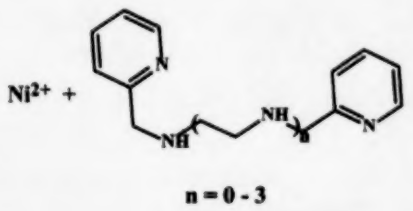

Eric D.A. Stemp, R. Erik Holmlin, Jacqueline K. Barton

Inorg. Chim. Acta 297 (2000) 88

Electron transfer between metal complexes bound to DNA: variations in sequence, donor, and metal binding mode

Photoinduced electron transfer from DNA-bound $M(phen)_2dppz^{2+}$ (dppz = dipyridophenazine, M = Ru or Os) to $Rh(phi)_2bpy^{3+}$ (phi = 9,10-phenanthrenequinone diimine) and $Ru(NH_3)_6^{3+}$ was studied as a function of DNA sequence. $Rh(phi)_2bpy^{3+}$ an intercalator, and $Ru(NH_3)_6^{3+}$, a groove-bound reactant, show opposite trends for quenching of DNA-bound $M(phen)_2dppz^{2+}$. We attribute the difference in reactivity among the DNA polymers to differences in how well the $M(phen)_2dppz^{2+}$ donor stacks in the DNA.

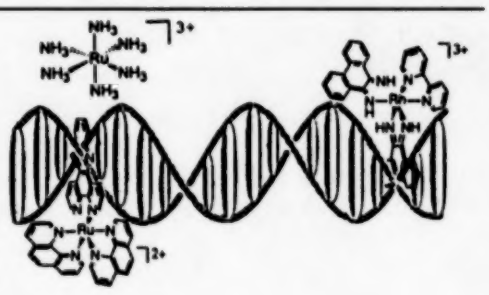

Kevin P. Maresca, Frank J. Femia, Grant H. Bonavia, John W. Babich, Jon Zubieta

Inorg. Chim. Acta 297 (2000) 98

Cationic complexes of the '3 + 1' oxorhenium–thiolate family

The reaction of $[Bu_4N][ReOBr_4(OPPh_3)]$ with $HSCH_2CH_2SCH_2CH_2SH$ yields $[ReOBr\{(SCH_2CH_2)_2S\}]$, a material which serves as a precursor for the preparation of a series of cationic '3 + 1' oxorhenium(V) thiolates. The reactions of $[ReOBr\{(SCH_2CH_2)_2S\}]$ with the appropriate thiolate ligands yields the complexes $[ReO\{(SCH_2CH_2)_2S\}(C_5H_4NH\text{-}4\text{-}S)]Br$ and $[ReO\{(SCH_2CH_2)_2S\}(SCH_2CH_2\text{-}NH_3)]Cl$.

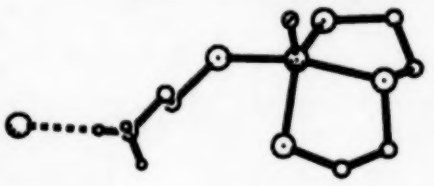

Dana S. Marlin, Marilyn M. Olmstead, Pradip K. Mascharak

Inorg. Chim. Acta 297 (2000) 106

Chemistry of iron(III) complexes of *N,N'*-bis(2-hydroxyphenyl)-pyridine-2,6-dicarboxamide: seven-coordinate iron(III) complexes ligated to deprotonated carboxamido nitrogens

The designed ligand $POPYH_4$, in its deprotonated form, employs two carboxamido nitrogens, one pyridine nitrogen, and two phenolate oxygen donors to bind Fe(III) and gives rise to seven-coordinate (pentagonal bipyramid) complexes of the type $[Fe(POPY)L_2]^{n-}$. It also affords the tetrahedral bis complex $[Fe(POPYH_2)_2]^-$ in which only phenolate oxygens of the ligand are bound to Fe(III).

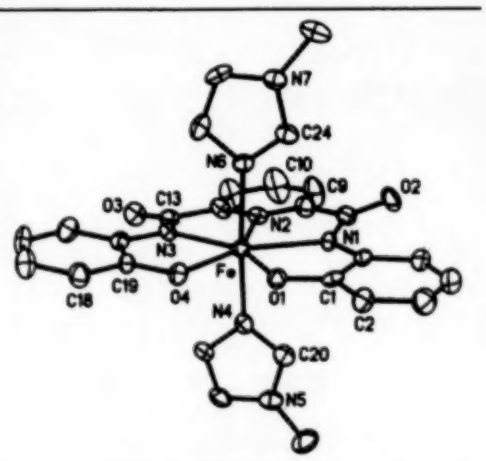

Lisa M. Berreau, Jason A. Halfen, Victor G. Young Jr., William B. Tolman

Inorg. Chim. Acta 297 (2000) 115

Heterocyclic donor influences on the binding and activation of CO, NO, and O_2 by copper complexes of hybrid triazacyclononane–pyridyl ligands

A series of Cu(I) complexes of ligands comprising 1,4-diisopropyl-1,4,7-triazacyclononane appended to variably substituted pyridyl or quinolyl donors have been characterized and their reactions with CO, NO, and O_2 explored. Interesting similarities and differences in the Cu(I)-small molecule chemistry compared to that exhibited by complexes ligated by the η^3- or η^4-binding counterparts R_3TACN (TACN = 1,4,7-triazacyclononane) or tris(pyridylmethyl)-amine, respectively, were observed.

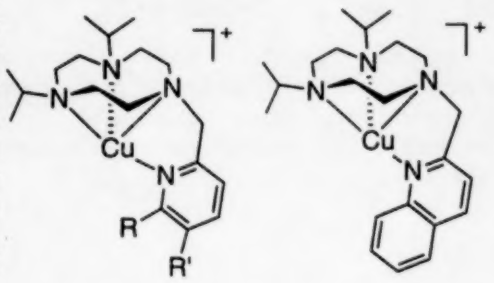

María Elba Quiroz-Castro, Gerard A. van Albada, Ilpo Mutikainen, Urho Turpeinen, Jan Reedijk

Inorg. Chim. Acta 297 (2000) 129

The crystal structure, spectroscopy and EPR of tetragonal bis(2-(aminomethyl)pyridine)Cu(II) compounds. Rare cases of the absence of Cu(II) plasticity

A few cases of the absence of Cu(II) plasticity are described in the structure spectroscopy and EPR of bis(2-(aminomethyl)pyridine)Cu(II) compounds.

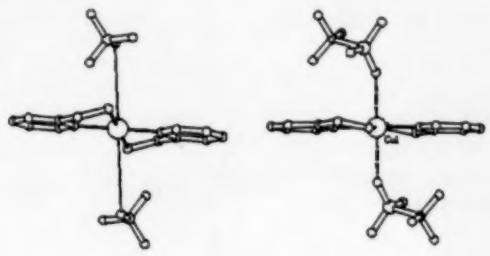

M. Kourgiantakis, M. Matzapetakis, C.P. Raptopoulou, A. Terzis, A. Salifoglou

Inorg. Chim. Acta 297 (2000) 134

Lead–citrate chemistry. Synthesis, spectroscopic and structural studies of a novel lead(II)–citrate aqueous complex

Reaction of $Pb(NO_3)_2$ with citric acid at low pH led to the synthesis of $[Pb(C_6H_6O_7)]_n \cdot nH_2O$ (**1**), the first Pb–citrate complex to be isolated from aqueous solutions. Complex **1** was structurally (X-rays) and spectroscopically (FT-IR) characterized and its behaviour as a function of pH explored. The study presents a first account of Pb–citrate species with potential relevance to biological Pb speciation and toxicity.

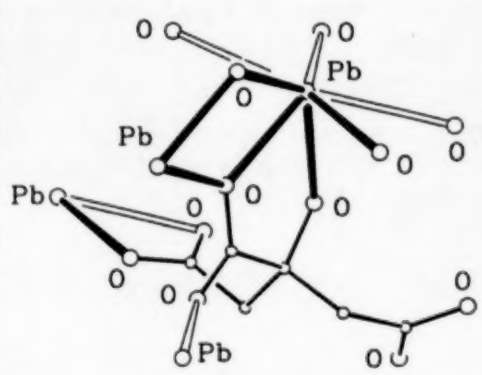

Etsuko Fujita, David J. Szalda

Inorg. Chim. Acta 297 (2000) 139

Crystallization and structure of a binuclear species containing the Co–C(OH)–O–Co moiety

The crystal structure of binuclear species containing the Co–C(OH)–O–Co moiety, $[(CoL)_2(COOH)](ClO_4)_3(NCCH_3)_2$ (L = 5,7,7,12,14,14-hexamethyl-1,4,8,11-tetraazacyclotetradeca-4,11-diene) is reported. Two $[CoL]^+$ units are bridged by a $COOH^+$. The carbon of the bridged $COOH^+$ is coordinated to one CoL^+ and the non-protonated oxygen to the other CoL^+ unit.

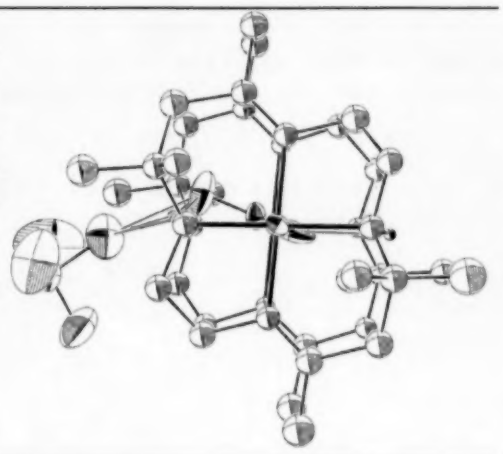

May Meroueh, Johan Kjellström, K.S. Margareta Mårtensson, Sofi K.C. Elmroth, Christine S. Chow

Inorg. Chim. Acta 297 (2000) 145

Reactions of platinum(II) complexes with a DNA hairpin, d(CGCGTTGTTCGCG): structural characterization and kinetic studies

Adduct formation between the complexes *cis*-$[Pt(NH_3)_2Cl(OH_2)]^+$, where R = H or C_6H_{11}, and the DNA hairpin d(CGCGTTGTTCGCG) was shown to take place preferentially at G7 in the hairpin loop. Platination results in the decrease of the melting temperature by approximately 11°C and formation of a DNA structure with pronounced salt dependence.

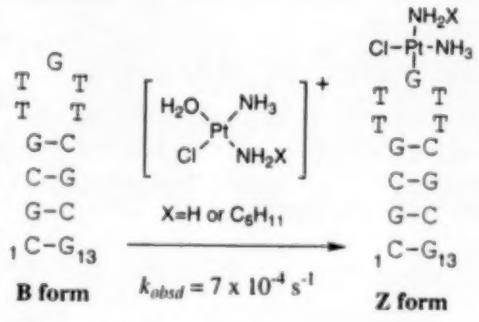

Grant M. Kloster, Stephen P. Watton

Inorg. Chim. Acta 297 (2000) 156

Oxidation of immobilized iron(II)-1,10-phenanthroline complexes by cerium(IV): a probe into the site accessibility of metal complexes covalently attached to silica sol–gels

The susceptibility of $[Fe(phen\text{-}R)_3]^{2+}$ complexes immobilized in sol–gel silica toward Ce(IV) oxidation was examined as a function of the number of covalent attachments between the complexes and the SiO_2 matrix. Unexpectedly, statistical analysis of the sigmoid response indicated that the oxidations may be affected by ligand dissociation processes. Isolation of inner-sphere oxidation products supports this conclusion.

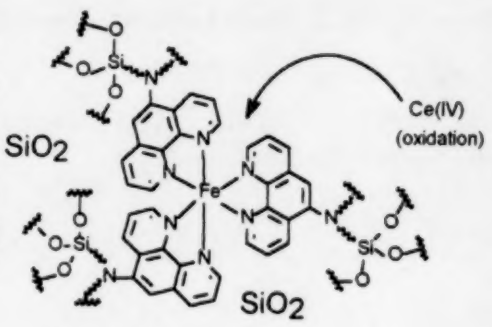

Tamako Ogihara, Shiro Hikichi, Munetaka Akita, Takeshi Uchida, Teizo Kitagawa, Yoshihiko Morooka

Inorg. Chim. Acta 297 (2000) 162

An approach to the O_2 activating mononuclear non-heme Fe enzymes: structural characterization of Fe(II)–acetato complex and formation of alkylperoxoiron(III) species with the highly hindered hydrotris(3-tert-butyl-5-isopropyl-1-pyrazolyl)borate

Structural characterization of an Fe(II)–acetato complex and attempts to synthesize mononuclear Fe(III) dioxygen complexes bearing the highly sterically demanding $Tp^{tBu,iPr}$ (=hydrotris(3-tertbutyl-5-isopropyl-1-pyrazolyl)borate) have been investigated. The extremely bulky $Tp^{tBu,iPr}$ ligand hinders the approach of the exogenous O_2 molecule to the coordinatively unsaturated Fe(II) centers. Reaction of $Tp^{tBu,iPr}$ (OH) with ^{t}BuOOH results in formation of a thermally unstable Fe(III)–alkylperoxo intermediate.

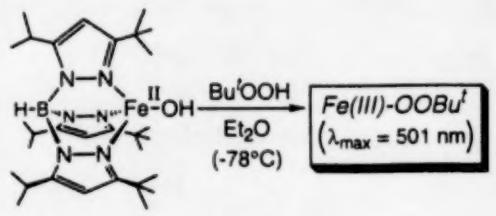

Erika R. Bauminger, Amyra Treffry, Michael A. Quail, Zhongwei Zhao, Israel Nowik, Pauline M. Harrison

Inorg. Chim. Acta 297 (2000) 171

Metal binding at the active centre of the ferritin of *Escherichia coli* (EcFtnA). A Mössbauer spectroscopic study

Mössbauer spectroscopy, Zn(II) and Tb(III) are used to study the relationship between iron oxidation intermediates in EcFtnA. We confirm the presence of two types of diiron dimers at the dinuclear centre of EcFtnA. An(II) is found to be an effective competitor for the dinuclear centre while Tb(III) is more effective at displacing iron from the third iron binding site (C).

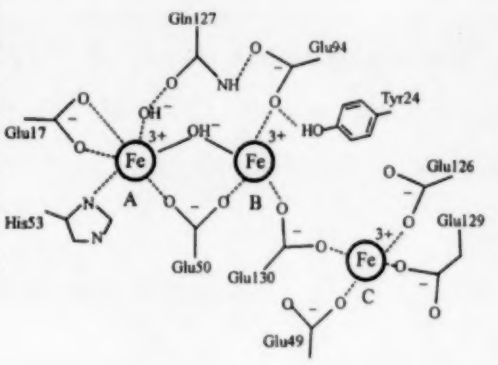

Eugenijus Urnėžius, Stephen J. Klippenstein, John D. Protasiewicz

Inorg. Chim. Acta 297 (2000) 181

Sterically promoted zirconium–phosphorus π-bonding: structural investigations of $[Cp_2Zr(Cl)\{P(H)Dmp\}]$ and $[Cp_2Zr\{P(H)Dmp\}_2]$ (Dmp = 2,6-$Mes_2C_6H_3$)

The new terminal zirconocene–organophosphanido complexes $[Cp_2Zr(Cl)\{P(H)Dmp\}]$ (**1**) and $[Cp_2Zr\{P(H)Dmp\}_2]$ (**2**) (Dmp = 2,6-$Mes_2C_6H_3$) bearing the sterically demanding ligand Dmp have been prepared and structurally characterized. A large range of geometries for the phosphorus atom of these complexes (pyramidal to planar) is observed. The Zr–P bond lengths for each phosphanido group decrease with the transformation from pyramidal to planar geometry.

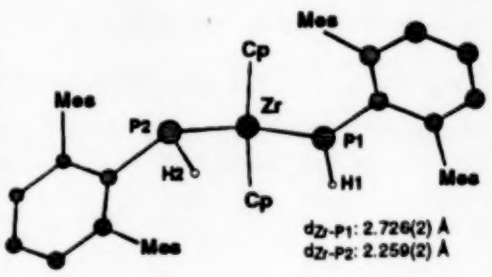

Emil V. Radkov, Robert H. Beer

Inorg. Chim. Acta 297 (2000) 191

A comprehensive series of Group 14 derivatives of the plenary mixed-metal polyoxometalate $[PNbW_{11}\text{-}O_{40}]^{4-}$

A homologous series of Group 14 derivatives of the mixed-metal Keggin ion $[LNbO]^{4-}$ ($L = \alpha\text{-}\{PW_{11}O_{39}\}7^-$) can be prepared in which the $\{Me_3E\}^+$ group (E = C Si, Ge, Sn, Pb) is bound selectively to the terminal ONb surface oxygen atom. Comparative multinuclear NMR spectroscopic and reactivity studies of $[LNbOE\text{-}Me_3]^{3-}$ reveal interesting similarities and differences within the series.

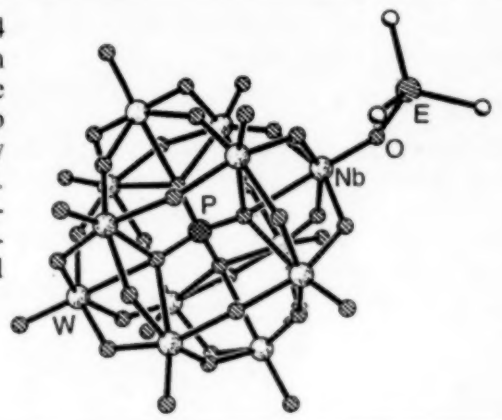

Ivano Bertini, Claudio Luchinat, Antonio Rosato

Inorg. Chim Acta 297 (2000) 199

The use of propionate α-proton contact shifts as structural constraints

The possibility of using the contact shifts of propionate α-protons as structural constraints for solution structure determination of low spin iron(III) hemoproteins is investigated. These constraints would be precious since the number of the NOEs for propionates can be small. Rat cytochrome b_5 is used as a test case.

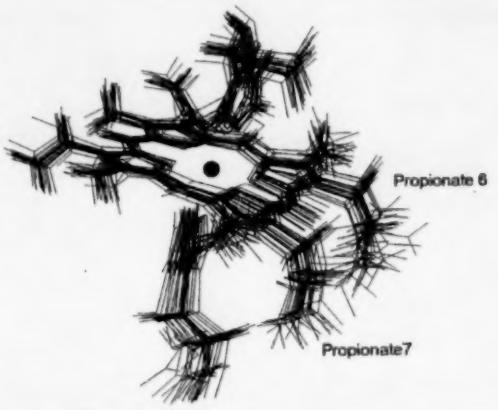

Benjamin W.F. Gordon, Michael J. Scott

Inorg. Chim. Acta 297 (2000) 206

Linked aryloxides ligands: synthesis and characterization of alkali metal clusters of a partial calix[n]arene

Much like the macrocycle calix[4]arene, intramolecular hydrogen-bonding interactions in the ligands 2,6-bis(3-tert-butyl-5-methyl-2-hydroxybenzyl)-4-methyl phenol (**L**) and 2,6-bis(3,5-ditert-butyl-2-hydroxybenzyl)-4-methyl phenol (**L'**) help orient the aryloxide donor atoms, and deprotonation of these groups with either sodium or lithium reagents affords unusual metal clusters. Depending on the donor properties of the solvent media, both tri- and hexametallic complexes can be isolated. In these clusters, the metal centers maintain extensive bridging interactions between aryloxide groups, and the *ipso*-carbon atom of the central aryloxide helps to stabilize unusual coordination environments around the metal centers.

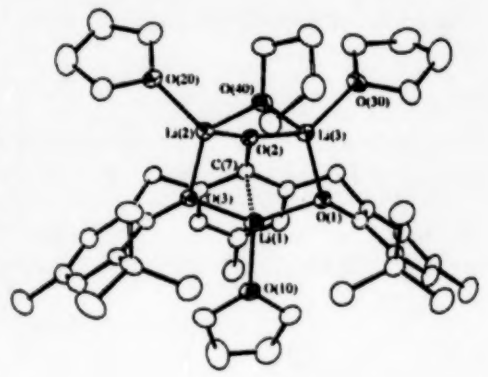

Jeffrey C. Buchsbaum, Jeremy M. Berg

Inorg. Chim. Acta 297 (2000) 217

Kinetics of metal binding by a zinc finger peptid

The kinetics of zinc(II) and cobalt(II) binding by a prototypical zinc finger peptide has been examined. Differences in the second-order rate constants for metal binding and in the first-order rate constants for metal dissociation contribute about equally to the observed 10^4-fold thermodynamic preference for zinc(II) over cobalt(II) characteristic of these peptides. The exchange of zinc(II) for cobalt(II) occurs by a dissociative mechanism. The level of kinetic preference for zinc(II) over cobalt(II) binding is comparable to that seen for other zinc metalloproteins despite large differences in absolute rate.

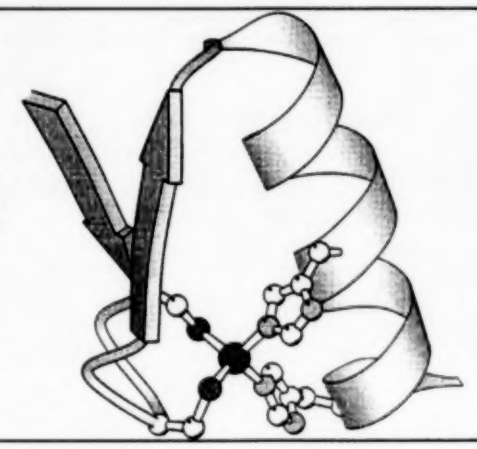

Jasper McCrea, Vickie McKee, Ted Metcalfe, Santokh S. Tandon, Jan Wikaira

Inorg. Chim. Acta 297 (2000) 220

Geometric control of redox level in tetranuclear manganese and cobalt systems

The observed redox levels of a series of mixed-valence tetranuclear manganese and cobalt complexes are accounted for by geometric constraints transmitted from one metal ion to the next through the ligand framework, providing a basis for cooperative control of redox processes. Similar dynamic mechanisms are likely to apply in polynuclear redox-active metalloenzymes.

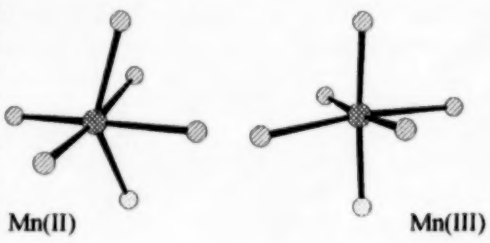

Eric D. Coulter, Neeta V. Shenvi, Zanna M. Beharry, Jennifer J. Smith, Benet C. Prickril, Donald M. Kurtz Jr.

Inorg. Chim. Acta 297 (2000) 231

Rubrerythrin-catalyzed substrate oxidation by dioxygen and hydrogen peroxide

Investigations were undertaken aimed at clarifying the reactivities of the $Fe(SCys)_4$ and diiron–oxo sites of rubrerythrin (Rr) during its catalysis of substrate oxidations by either O_2 or H_2O_2. The NADH peroxidase reaction: $NADH + H^+ + H_2O_2 \rightarrow NAD^+ + 2H_2O$, gave the highest turnover numbers. The results indicate that electrons from NADH flow initially into the $Fe(SCys)_4$ site of Rr, then out through the diferrous site into H_2O_2. An extra carboxylate ligand (Glu97) not present in other diiron–oxo enzymes may shift the reactivity of Rr towards H_2O_2 and away from O_2.

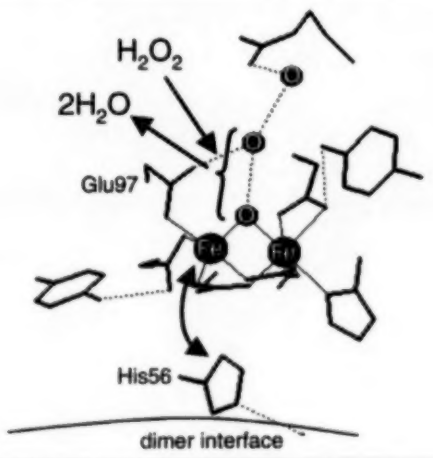

Elizabeth C. Theil, Hidenori Takagi, G. William Small, L. He, A.R. Tipton, D. Danger

Inorg. Chim. Acta 297 (2000) 242

The ferritin iron entry and exit problem

The control of iron and oxygen chemistry by the ferritin protein is discussed in terms of recent spectroscopic (Mössbauer, resonance Raman, UV–Vis) and protein crystallization data related to five Fe binding sites: (1) Fe^{2+} entry, (2) oxidation to diferric peroxo; (3) translocation of the peroxo decay products, the diferric oxo/hydroxo biomineral precursors to the mineralization cavity; (4) the mineral anchor site; and (5) the Fe exit site. New data include effects of tyrosine engineering and pH on site 2, building a new site 2, and engineering site 4 with cysteine or alanine. As many as 4500 Fe^{2+} atoms can be mineralized in a single protein molecule (molecular weight: 480 kDa, assembled from 24 subunits.)

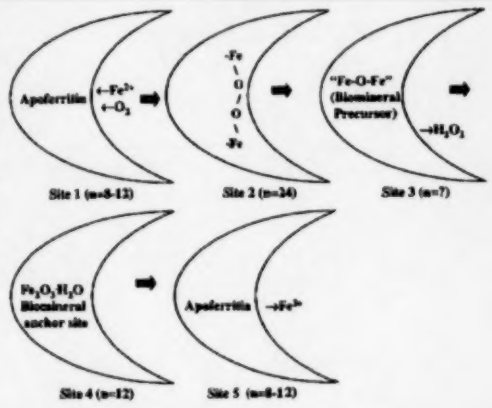

Neil A. Law, Jeff W. Kampf, Vincent L. Pecoraro

Inorg. Chim. Acta 297 (2000) 252

A magneto-structural correlation between the Heisenberg constant, *J*, and the Mn–O–Mn angle in $[Mn^{IV}(\mu\text{-}O)]_2$ dimers

This contribution presents the magneto-structural correlation between the Mn–O–Mn angle of high-valent manganese dimers with the $[Mn^{IV}\ (\mu\text{-}O)]_2$ core motif and the Heisenberg coupling constant, *J*. The implications of these data for the oxygen evolving complex are discussed. In addition to this correlation, we describe two new and unique structures for the dimers $[Mn^{IV}$-(3,5-di-*t*-busalpn)$(\mu\text{-}O)]_2$ and $[Mn^{IV}$(3,5-di-Cl-salpn)$]_2$.

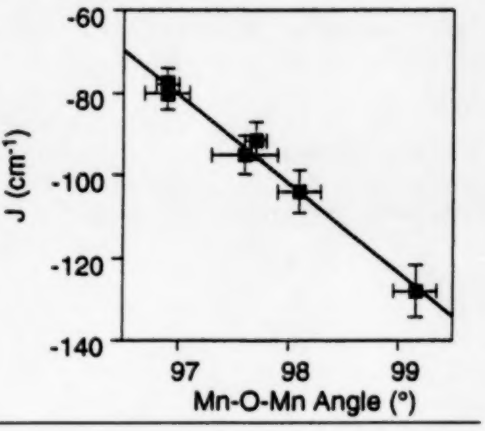

Jochen Müller, Akihiro Kikuchi, Eckhard Bill, Thomas Weyhermüller, Peter Hildebrandt, Linda Ould-Moussa, Karl Wieghardt

Inorg. Chim. Acta 297 (2000) 265

Phenoxyl radical complexes of chromium(III), manganese(III), cobalt(III), and nickel(II)

A number of relatively stable octahedral complexes of $M = Ga^{II}$, Cr^{III}, Ni^{II} containing a coordinated *phenoxyl radical* have been prepared from their corresponding phenolate analogs in solution. Electronic, resonance Raman and EPR spectra prove unambiguously that the phenoxyl radical is *O*-coordinated to the corresponding metal ion. The electronic ground state of these species with a paramagnetic metal ion (d^n, $n = 3,4,8$) and a ligand radical ($S = 1/2$) has been determined. Depending on the d^n configuration of the metal ion anti- and ferromagnetic intramolecular coupling had been established.

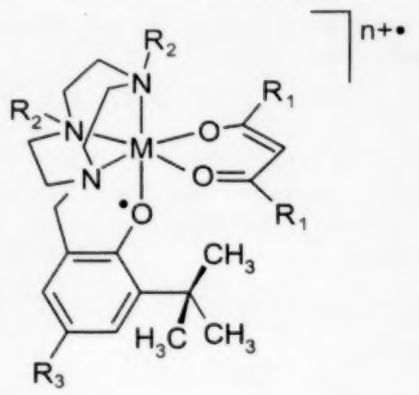

Serena DeBeer, Pernilla Wittung-Stafshede, Johan Leckner, Göran Karlsson, Jay R. Winkler, Harry B. Gray, Bo G. Malmström, Edward I. Solomon, Britt Hedman, Keith O. Hodgson

Inorg. Chim. Acta 297 (2000) 278

X-ray absorption spectroscopy of folded and unfolded copper(I) azurin

The structure of the copper site in folded and unfolded copper(I) azurin has been investigated by X-ray absorption spectroscopy (XAS). The lengths of both the Cu–S(Cys) and Cu–N(His) bonds increase by ~0.1 Å on unfolding, in accord with the view that copper coordination is constrained by the protein.

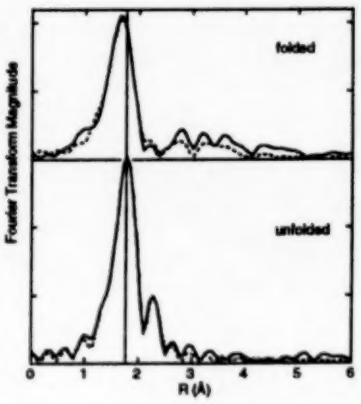

Tong Ren, Chun Lin, Edward J. Valente, Jeffrey D. Zubkowski

Inorg. Chim Acta 297 (2000) 283

The influence of remote substituent in tetrakis-(μ-*N*,*N*′-diarylformamidinato)–dirhodium(II) compounds.
Part 7. Linear free energy relationships in dinuclear compounds

A series of tetrakis(μ-*N*,*N*′-diarylformamidinato)dirhodium(II) compounds was synthesized and characterized, where aryl is either XC_6H_4- with substituent X as *p*-OMe, *p*-Me, H, *m*-OMe, *p*-Cl, *m*-Cl, *m*-CF_3, *p*-CF_3, or 3,4-$Cl_2C_6H_3$, or 3,5-$Cl_2C_6H_3$. Excellent Hammett correlation was established between the substituent constant (σ) and the electrode potentials of quasireversible redox couples Rh_2^{6+}/Rh_2^{5+} (**A**), Rh_2^{5+}/Rh_2^{4+} (**B**), and Rh_2^{4+}/Rh_2^{3+} (**C**), as indicated by the linear plots shown on the right.

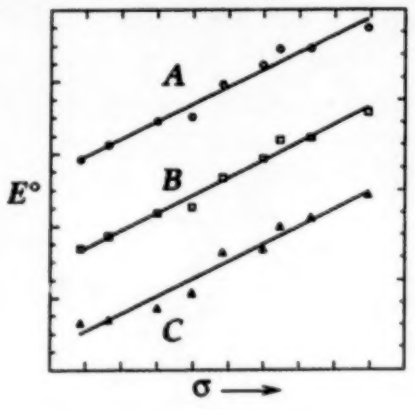

G.L. Abbati, A. Caneschi, A. Cornia, A.C. Fabretti, D. Gatteschi

Inorg. Chim. Acta 297 (2000) 291

$[Fe(OCH_3)_2(dbm)]_{12}$: synthesis, solid-state characterization and reactivity of a new molecular ferric wheel

A full control of the reactivity of transition metal clusters can be achieved by exploiting template effects: the twelve-membered iron(III) ring $[Fe(OCH_3)_2(dbm)]_{12}$ spontaneously halves in the presence of Li^+ or Na^+ templates in organic solution to give six-membered rings which entrap an alkali-metal iron.

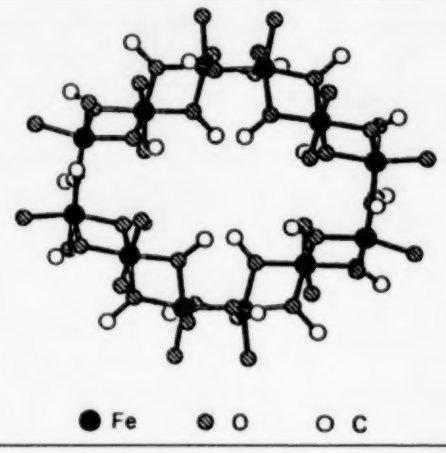

Julian Limburg, Robert H. Crabtree, Gary W. Brudvig

Inorg. Chim. Acta 297 (2000) 301

Kinetic analysis of the O_2-forming reaction between $[Mn(III)(dpa)_2]^-$ (dpa = dipicolinate) and potassium peroxomonosulfate

When $[Mn(dpa)_2]^-$ is added to a solution containing excess $KHSO_5$, O_2 is evolved. The reaction is initiated by the formation of $[(H_2O)(dpa)Mn(O)_2Mn(dpa)(OH_2)]^-$, and ends with the irreversible conversion of the catalyst to MnO_4^-. A kinetic analysis of these reactions is reported along with a proposed mechanism that involves a MnV=O containing intermediate.

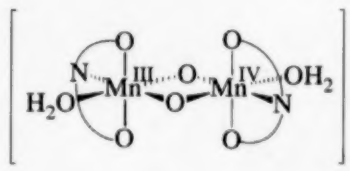

Jungseok Heo, Jaheon Kim, Dongmok Whang, Kimoon Kim

Inorg. Chim Acta 297 (2000) 307

Columnar one-dimensional coordination polymer formed with a metal ion and a host–guest complex as building blocks: potassium ion complexed cucurbituril

Cucurbituril, a barrel-shaped molecule and potassium ion form a columnar 1D coordination polymer in the solid state, formula of which is $[(C_{36}H_{36}N_{24}O_{12})K_2(OH)_2 \cdot (C_4H_8O)]_n$. In the coordination polymer, cucurbituril molecules stack atop one another through coordination of their carbonyl groups to the potassium ions in between. A disordered THF molecule is encapsulated in the cavity of each of the cucurbituril molecule.

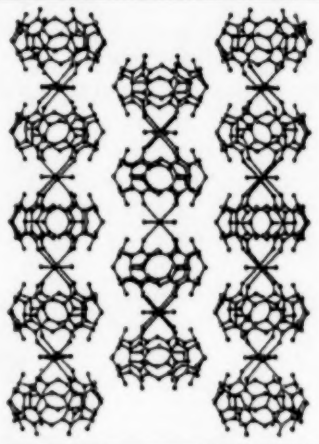

Subhasish Mukerjee, Kirsten Skogerson, Susan DeGala, John P. Caradonna

Inorg. Chim. Acta 297 (2000) 313

Skirting the oxo-wall: characterization and catalytic reactivity of binuclear $Co^{2+/3+}$ 1,2-bis(2-hydroxybenzamido)benzene complexes with comparison to their isostructural $Fe^{2+/3+}$ analogs. Implications of d-electron count on oxygen atom transfer catalysis

A comparison of the structural, spectroscopic, and catalytic oxygen atom transfer properties of iron and cobalt based binuclear complexes of the type $[M_2^{2+}(H_2Hbab)_2(N\text{-MeIm})_2]$ (H_4Hbab = 1,2 - bis(2 - hydroxybenzamido)benzene) is reported. The mechanistic implications of the significantly different product distributions obtained with the Co^{2+} (d^7) dimer versus the isostructural Fe^{2+} (d^6) dimer are presented and discussed. These data strongly infer the operation of two independent mechanisms for the Co^{2+} and Fe^{2+} catalyzed reactions.

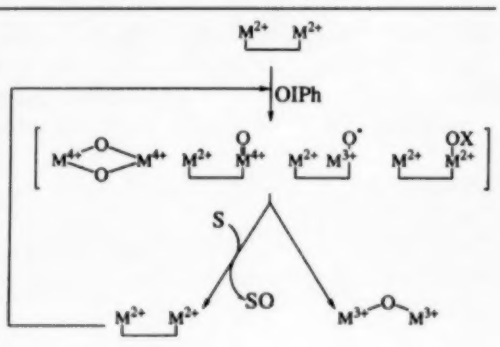

Aaron L. Odom, Alan F. Heyduk, Daniel G. Nocera

Inorg. Chim. Acta 297 (2000) 330

Photochemistry of dirhodium(II,II) diphosphazane tetrachloride complexes

The complex $Rh_2(PP)_3Cl_4$ (PP = $MeN(PF_2)_2$) undergoes four-electron reductive elimination when irradiated with near-UV light. The reaction was found to proceed in sequential two-electron steps: from $Rh_2(PP)_3Cl_4$ to $Rh_2(PP)_3Cl_2(\eta^1\text{-PP})$ to $Rh_2(PP)_3(\eta^1\text{-PP})_2$, with individual quantum yields of 0.05(1) and 0.006(2). The sterically more encumbered complex, $Rh_2\{MeN[P(OEt^{F3})_2]_2\}_3Cl_4$ ($MeN[POEt^{F3})_2]_2$ = $MeN[P(OCH_2CF_3)_2]$), reacts by a completely different mechanism.

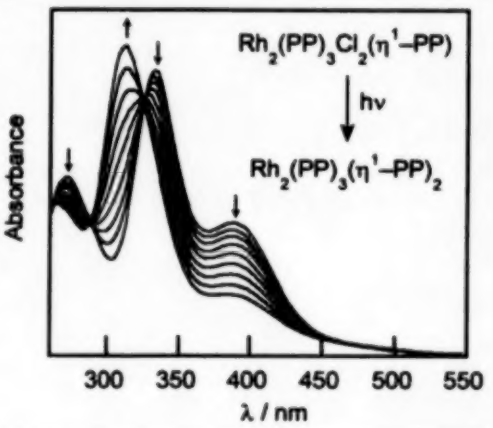

Irène Morgenstern-Badarau, François Lambert, Jean Philippe Renault, Michèle Cesario, Jean-Didier Maréchal, Feliu Maseras

Inorg. Chim. Acta 297 (2000) 338

Amine conformational change and spin conversion induced by metal-assisted ligand oxidation: from the seven-coordinate iron(II)–TPAA complex to the two oxidized iron(II)–$(py)_3$tren isomers. Characterization, crystal structures, and density functional study

The tripodal heptadentate ligand TPAA (TPAA = tris[*N*-(2-pyridylmethyl)-2-amino-ethyl]amine) is found to undergo an iron(II)-assisted oxidative dehydrogenation with its three amine functions oxidized into three imine groups, giving the tripodal potentially heptadentate ligand $(py)_3$tren ($(py)_3$tren = tris[*N*-(2-pyridylmethyl)-2-iminoethyl]amine). This oxidative process induces structural changes and spin conversion in the three identified iron(II) complexes, Fe–TPAA complex (**1**), Fe–py3tren complexes (**2**) and (**3**). X-ray crystallographic studies revealed differences in the coordination geometry of the bridging nitrogen atom and shifts in the coordination number from seven to six. Spin alteration is observed from the high-spin complex **1** to the low-spin complex **3** while its isomeric form, the intermediate complex **2** exhibits a temperature-dependent spin conversion. DFT calculations carried out on two isomeric complexes **2** and **3** are also reported.

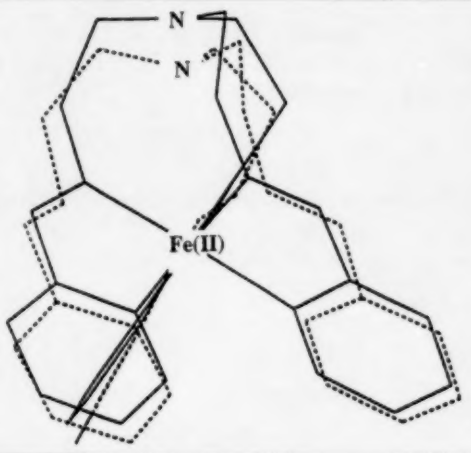

Michael Kavana, Douglas R. Powell, Judith N. Burstyn

Inorg. Chim. Acta 297 (2000) 351

Static versus dynamic Jahn–Teller distortions in octahedral-like copper(II) complexes of 1,4,7-triazacyclononane and 1-oxa-4,7-diazacyclononane: implications for hydrolytic reactivity

Characterization by X-ray crystallography, EPR, and electronic absorption spectroscopy is reported for $[Cu([9]aneN_3)_2][CF_3SO_3]_2 \cdot H_2O$, $[Cu([9]aneN_2O)_2][BF_4]_2$, and $[Cu([9]aneN_2O)_2][NO_3]_2$. Dynamic Jahn–Teller distortion present in the $Cu([9]aneN_3)_2^{2+}$ cation is removed upon replacement of one nitrogen donor with oxygen. The absence of dynamic distortion in complexes of [9]aneN_2O correlates with a lowered reactivity for phosphodiester hydrolysis, suggesting that ligand fluxionality may be important in Cu(II)-promoted hydrolysis.

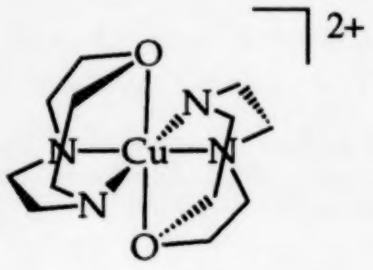

Telvin D. Ju, Amina S. Woods, Robert J. Cotter, Pierre Moënne-Loccoz, Kenneth D. Karlin

Inorg. Chim. Acta 297 (2000) 362

Dioxygen and nitric oxide reactivity of a reduced heme/non-heme diiron(II) complex $[(^5L)Fe^{II}\cdots Fe^{II}–Cl]^+$. Using a tethered tetraarylporphyrin for the development of an active site reactivity model for bacterial nitric oxide reductase

Reactivity models for the active site in NO reductase, $[(^5L)Fe^{II}\cdots Fe^{II}–Cl]^+$ (**2**), have been synthesized. Reaction with O_2 gives a -80°C stable intermediate; warming gives μ-oxo complex $[(^5L)Fe^{III}–O–Fe^{III}–Cl]^+$ (**1**). At low concentrations of **2**, reaction with $NO_{(g)}$ gives **1**; an intermediate (-80°C) is observable. Otherwise, a metal–nitrosyl complex forms ($\nu_{(N–O)} \sim 1660\ cm^{-1}$), with concomitant evolution of N_2O and NO_2 gases.

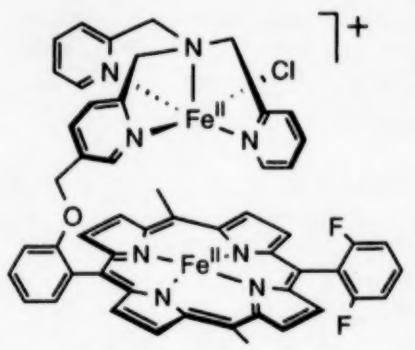

$[(^5L)Fe^{II}...Fe^{II}-Cl]^+$ (**2**)

Chebrolu P. Rao, K. Geetha, M.S.S. Raghavan, A. Sreedhara, K. Tokunaga, T. Yamaguchi, V. Jadhav, K.N. Ganesh, Thanuja Krishnamoorthy, Kolluru V.A. Ramaiah, R.K. Bhattacharyya

Inorg. Chim. Acta 297 (2000) 373

Transition metal saccharide chemistry and biology: syntheses, characterization, solution stability and putative bio-relevant studies of iron–saccharide complexes

A number of iron–saccharide complexes having high water solubility and good hydrolytic stability were synthesized and characterized extensively using analytical, spectral, magnetic and electrochemical studies. Number of iron centers present in these complexes differed. These have exhibited reductive release of iron in a controlled fashion and have shown efficient transport through membranes. Furthermore, these can complement the deficiency of hemin in lysate.

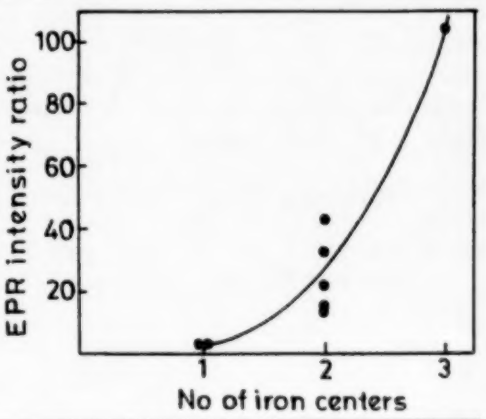

Sergiu M. Gorun, Zhengbo Hu, Robert T. Stibrany, Gene Carpenter

Inorg. Chim. Acta 297 (2000) 383

Synthesis and molecular structures and oxidation catalysis of mixed alkyl, fluoroalkyl pyrazolylborate metal complexes

Cobalt (**1a**), manganese (**1b**) and copper (**2**) complexes of partially fluorinated tris- and bispyrazolyl borates, respectively, were prepared. The formally square–planar **2** exhibits long Cu···H axial contacts. In contrast, the fluorine-lined cavities surrounding the cobalt and manganese allow the metals to reach six-coordination by accommodating small molecules at potentially open coordination sites. **1a** catalytically decomposes cumyl hydroperoxides to oxygenate cyclohexane to cyclohexanol and cyclohexanone 50% faster relative to its non-fluorinated analogue.

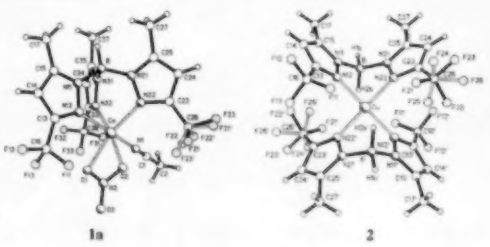
1a 2

Euan K. Brechin, Michael J. Knapp, John C. Huffman, David N. Hendrickson, George Christou

Inorg. Chim. Acta 297 (2000) 389

New hexanuclear and octanuclear iron(III) oxide clusters: octahedral $[Fe_6O_2]^{14+}$ species and core isomerism in $[Fe_8O_4]^{16+}$ complexes

New hexanuclear and octanuclear structural types in iron(III) cluster chemistry have been prepared from the reactions of 2-(hydroxymethyl)pyridine (hmpH) with Fe(III) reagents in the presence of carboxylate ions. The hexanuclear species $[Fe_6O_2(O_2CR)_6(hmp)_6]^{2+}$ contain an Fe_6 octahedron whereas the octanuclear species $[Fe_8O_4(O_2CPh)_{11}(hmp)_5]$ and $[Fe_8O_4(O_2CMe)_{12}(hmp)_4]$ have a more extended structure and possess *syn* and *anti* isomeric forms, respectively, of the $[Fe_8O_4]$ core. Both the Fe_6 and Fe_8 cluster types possess $S=0$ ground states, consistent with predominantly antiferromagnetic exchange interactions between the constituent metal ions.

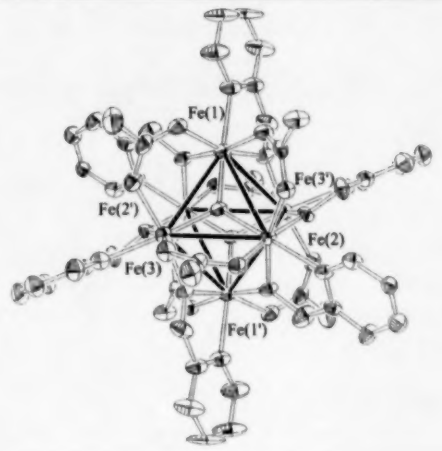

Peter E. Doan, Brian M. Hoffman

Inorg. Chim. Acta 297 (2000) 400

How important is parallel-mode EPR in electron spin echo envelope modulation studies of non-Kramers systems?

The EPR spectra of 'non-Kramers (NK) doublets' are commonly recorded using specially-constructed parallel-mode spectrometers rather than traditional EPR spectrometers. The efficacy of parallel and perpendicular ESEEM spectroscopy on the NK-doublet of azido-hemerythrin (N_3Hr_{red}) are compared. These results demonstrate that for this technique, the advantages of parallel-mode over perpendicular-mode ESEEM are minimal at best.

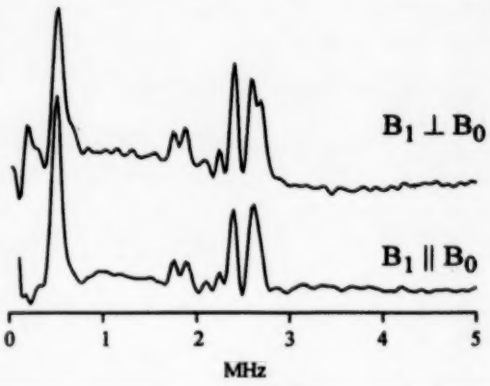

Duncan Odom, Christine J. Gramer, Victor G. Young Jr., Scott A. Hilderbrand, Suzanne E. Sherman

Inorg. Chim. Acta 297 (2000) 404

Synthesis and characterization of magnesium and zinc complexes of 1,4,7-triazacyclononane-*N*-acetate. Potential models for the active site of RuBisCo

Zinc and magnesium complexes of the tetradentate pendant-arm macrocycle 1,4,7-triazacyclononane-*N*-acetate (L) were synthesized and characterized by single-crystal X-ray crystallography. The complex cation of $[ZnL(H_2O)]O_3SCF_3{\cdot}C_2H_5OH$ (**1**) forms a polymeric chain with zinc centers bridged in a *syn*, *anti* fashion by acetate pendant arms. The complex cation of $[MgL(H_2O)_2]O_3SCF_3$ (**2**) is mononuclear, with two adjacent coordination sites on magnesium occupied by water molecules. These labile coordination sites may provide a binding site for activation of substrates in functional modeling of magnesium enzymes such as RuBisCo.

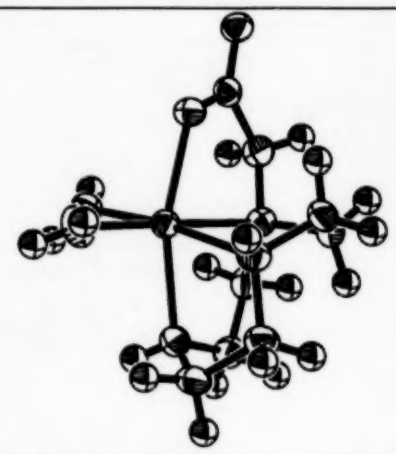

Notes

Sheila M. Morehouse, Huda Suliman, Janet Haff, Dao Nguyen

Inorg. Chim. Acta 297 (2000) 411

The structure and electrochemistry of imidazolebis-(1-10 phenanthroline)copper(II) nitrate

The structure consists of discrete $[Cu(phen)_2(imidazole)]^{2+}$ ions with a distorted square pyramidal geometry about the copper. One of the *cis*-phenanthroline ligands is asymmetrically coordinated to the axial ($Cu–N_{im} = 1.980(6)$) and equatorial ($Cu–N_{phen} = 2.050(5)$ Å) sites, while the second phenanthroline ($Cu–N_{phen} = 2.027(5)$ and 2.021(5) Å) and the imidazole ($Cu–N_{im} = 1.980(6)$ Å) occupy the remaining equatorial sites. The reversible one-electron reduction potential of $[Cu(phen)_2(imidazole)]^{2+}$ ($E_{1/2} = 0.10$ V) in methanol is more negative than that observed for $[Cu(phen)_2(NO_3)]_2$ ($E_{1/2} = 0.16$ V).

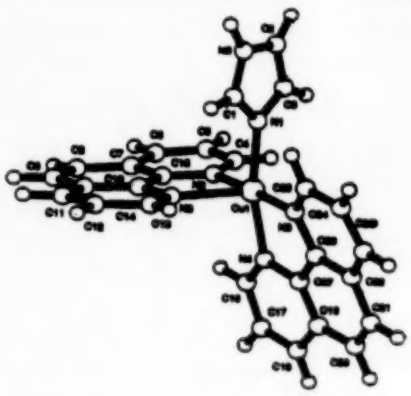

Miguel-Angel Elizondo-Riojas, Jiří Kozelka

Inorg. Chim. Acta 297 (2000) 417

Asymmetrical complexes $[Pt(N,N\text{-dmen})(dGuo)L]^{(2)+}$ (*N*,*N*-dmen = *N*,*N*-dimethylethylenediamine; L = H_2O, Cl^-, dGuo): H8 nuclei experience an orientation-dependent deshielding effect attributable to the paramagnetic anisotropy of the platinum atom

In the NMR spectrum of the isomer **Ib** of $[Pt(N,N\text{-dmen})(dGuo)^{2+}$, the guanine H8 proton resonates ~0.3 ppm downfield compared to **Ia**. We attribute this difference to different orientations of the guanines: roughly perpendicular to the square plane in **Ib** and oblique in **Ia**. The perpendicular orientation in **Ib** approaches H8 to the *z*-axis, where it experiences deshielding due to paramagnetic anisotropy.

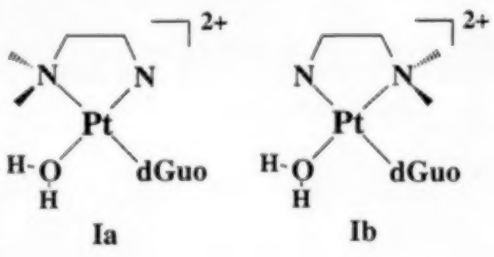

Conference Calendar 421
Author Index of Volume 297 425

The publisher encourages the submission of articles in electronic form thus saving time and avoiding rekeying errors. Please refer to the online version of the Guide for Authors at http://www.elsevier.nl/locate/ica

CONTENTS direct

This journal is part of **ContentsDirect**, the ***free*** alerting service which sends tables of contents by e-mail for Elsevier Science books and journals. You can register for **ContentsDirect** online at: **www.elsevier.nl/locate/contentsdirect**

http://ChemWeb.com
The World Wide Club for the Chemical Community
http://chemweb.com/gateways/elsevier.html